Development of a Moving Magnet Linear Motor Pressure Wave Generator for a Pulse Tube Refrigerator

S. Jacob[1], V. Ramanarayanan[1], R. Karunanithi[1], C.Damu[1], G. Jagadish[1], M.Achanur[1], R. Manjunatha[1], R.S. Prabhu[2], J. Kranthi Kumar[1], A. Gour[1] and A. S. Gaunekar[2]

[1]Indian Institute of Science, Bangalore, India 560012.
[2]ASM Technology Singapore Pte Ltd, Singapore 768924.

ABSTRACT

A pressure wave generator (PWG) is the most critical component of a high frequency pulse tube cooler which is finding increased use in aerospace and ground applications, including the telecommunication sector. High efficiency, compactness, low weight, high reliability and low vibration are some of the most challenging attributes in its design. This paper describes the developmental studies of a moving magnet linear motor PWG of 2 cc swept volume with a dual opposed piston configuration. The generative and restoring force characteristics of the magnetic circuit have been evaluated using a force measurement set up. Spiral arm flexures have been designed using FEM, fabricated and qualified by test. The linear motors alone are tested under resonant conditions without gas spring forces to estimate the iron losses of the motors. The influences of coil wire cross-section and number of coil turns on the performance of the PWG have been studied experimentally. The paper describes the significant effect of compressor flow discharge line cross section on the efficiency of the system. The performances of the PWG at different gas fill pressures and operating frequencies have been investigated. With an input power of 35.2 W, the PWG has produced a shaft power of 26.8 W and an acoustic power of 18.7 W.

INTRODUCTION

Lightweight, compact, and high frequency pulse tube coolers with high efficiency, high Mean Time To Failure (MTTF), and low vibration, are witnessing rapid growth for aerospace and ground applications. The most critical component of the cooler giving the above attributes is the linear motor pressure wave generator (compressor). A program has been initiated at our Institute to develop necessary expertise in the design, fabrication and testing of high frequency pulse tube coolers, including linear motor compressor. This paper presents the initial effort of our research group to design, develop and test a 2 cc swept volume moving magnet, dual opposed linear motor compressor.

DESIGN CHALLENGES

Electrical and Magnetic Considerations

Moving magnet technology is preferred to moving coil technology due to the distinct advantages of the former by avoiding flying leads, contamination of working helium gas from coil potting

Cryocoolers 16, edited by S.D. Miller and R.G. Ross, Jr.

components and a nonmetallic seal to take out power leads from the coils. However, placing the coil and outer yoke external to the pressure vessel will lower motor efficiency because of increased air gap in the magnetic circuit, which calls for optimized design, precision fabrication and assembly. Also, the iron losses in moving magnet configuration can be higher as compared to moving coil systems due to the exposure of magnets and compressor components to the changing magnetic field, whereas in moving coil systems, only the coil and coil holder are subjected to the changing magnetic field. This necessitates the use materials with low electrical conductivity and with high structural strength such as Titanium and requires efforts to optimize their volume. The yoke materials should have low hysteresis and eddy losses. Thus, it is imperative to design with low piston stroke amplitude (increased piston diameter consequently). Since hysteresis losses are proportional to frequency while eddy losses are proportional to the square of the frequency, the operating frequency has to be chosen with due diligence. A major loss in a linear motor is due to copper losses and, therefore, the coil wire diameter and coil length are to be optimized with respect to the needed generative force. To improve the packing density of coil winding, which has a large bearing on the diameter of the outer yoke and the motor weight, as well as to achieve enhanced heat transfer of the coil heat to the system sink, square copper wires of optimum gauges with high quality insulation have been selected.

For a linear motor with moving permanent magnet, the generative forces F is given by

$$F = B_g \cdot 2\, I_m \cdot L \tag{1}$$

where B_g is the magnetic flux density in the air gap between the yokes, L is the peripheral length of the magnet and I_m is equivalent current on either side of the magnets. Since B_g can only be increased by a higher coil current, which leads to higher I^2R losses, it is not an attractive option to increase the generative force. The addition of two side magnets to the main magnets can double the equivalent current of the magnetic circuit,[1,2] thus providing the possibility to double the generative force.

The magnets can be arranged on the magnetic holder as segmented magnet elements or as ring magnets. Radially-magnetized ring magnets facilitate easy assembly of the magnetic elements on the holder and provide a fail safe condition under shock and vibration. However, ring magnets demand uniform air gaps, which gives rise to unbalanced radial forces on the piston support system. This forces the need for precision fabrication and assembly. For the linear motor we have chosen Nd-Fe-B side and main magnet rings mounted on a Titanium magnet holder in S/N to N/S, and S/N to N/S polarity as shown in Fig. 1.

Generating Force and Restoring Force Measurements

For the experiments, three different wire sizes, 24 AWG, 21 AWG, and 18 AWG, are used for the coil winding. The outer and inner yokes are fabricated using the soft magnetic composite (SMC),

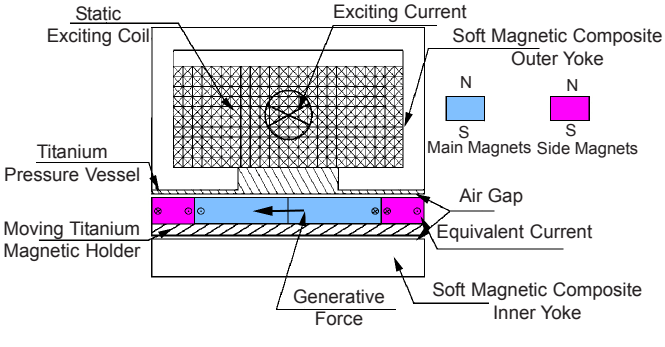

Figure 1. Schematic of magnetic circuit components

Somaloy (Höganäs, Sweden), which has low iron losses due to the high quality processing of surface insulated iron powder. The wires are wound directly on the titanium pressure vessel.

It is necessary to measure the generative and restoring force of the motor to optimize the number of turns and the operating parameters of the motor. A force measurement system has been designed and fabricated in the laboratory as shown in Fig. 2(a) and 2(b). The motor shaft (piston) is suspended from a force balance and counter weights are attached to the opposite side of the shaft to produce the necessary tension in the suspension string. By precision displacement of the shaft, the restoring force of the magnet is measured at zero current. Subsequently the current is supplied to the motor coil for different displacement values of the shaft and the resultant forces are measured.

The force displacement curve at different values of current for a 24 AWG 340 turn coil is shown in Fig. 3. The restoring force of the magnet assembly obtained from the measurement is about 9200 N/m.

Mechanical Configuration

Fig. 4 shows a picture of the moving magnet compressor. The two linear motors are connected to a central aluminum flange with an aligned central axis. This alignment cancels much of the on-axis vibration when the motors are run in the dual opposed configuration. The pressure vessel,

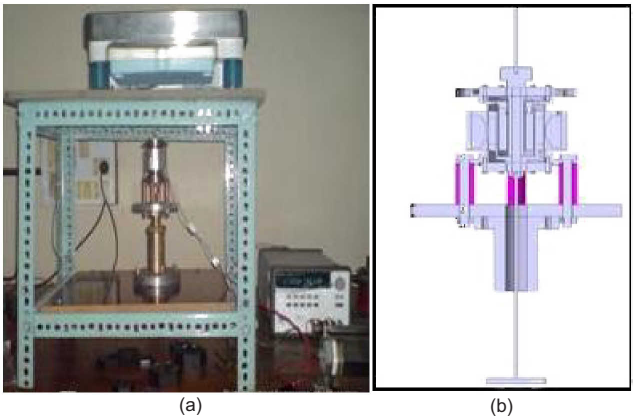

Figure 2. (a) Force measurement set up, (b) Schematic of the force measurement set up.

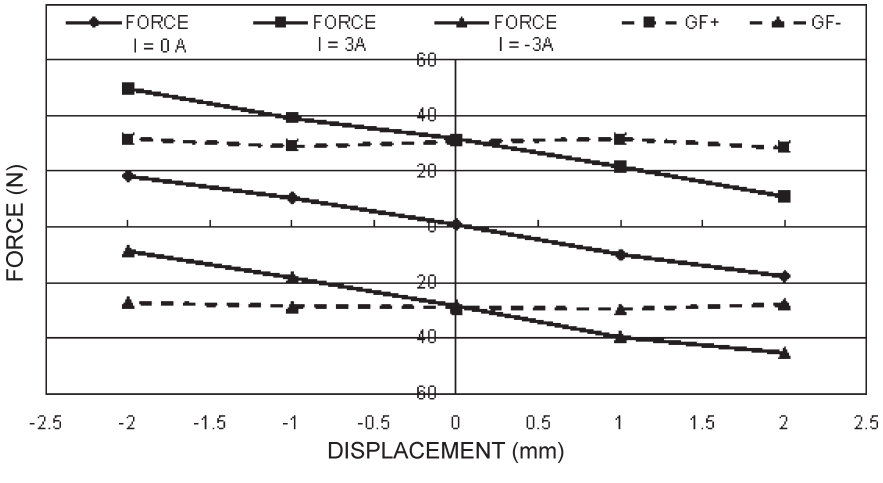

Figure 3. Variation of force with displacement at different values of current for a 340 turn coil.

piston cylinder, piston and magnetic holder are made of Ti-6Al-4V alloy.

The stress levels in the contours of the pressure vessel are optimized by FEM analysis to give a sufficient factor of safety for operation at up to a helium fill pressures of 30 bars. Each piston is supported in the front and rear by two sets of flexure stacks to provide a controlled clearance gap between the piston and cylinder. In order to reduce blowby losses at the clearance gap, an in-cylinder position contoured Rulon sleeve is fixed over the piston to achieve a close clearance. This seal clearance is maintained under dynamic conditions by the flexure stacks designed using the ANSYS® 10.0 FEM software package. A three spiral arm flexure design provides a high radial/axial stiffness. The flexure contours are optimized such that the Von Mises stress values are about 50% of the fatigue limit for the spring steel (Sandvik Sweden). The stress distribution in the flexure element is close to this limit as shown in Fig. 5. The ratio of radial stiffness to axial stiffness is shown in Table 1. Using modal analysis, the first natural frequency of the flexure is estimated to be 106 Hz. The flexure profiles are fabricated through photochemical etching.

The axial stiffness values of the flexures obtained by FEM analysis are verified experimentally by measuring deflection v/s load. The experimental axial stiffness value obtained is about 90% of FEM value. Finally the flexures are fatigue tested for 10^8 cycles at 1.25 times of the designated stroke. For the test, a linear motor configuration with an identical moving mass assembly of the operating system is used. The tests were carried out at 50 Hz frequency and no failure of the flexure stack was experienced during the tests.

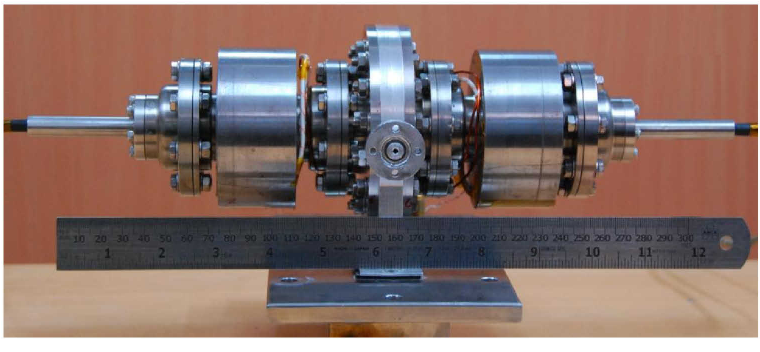

Figure 4. Moving magnet linear motor compressor

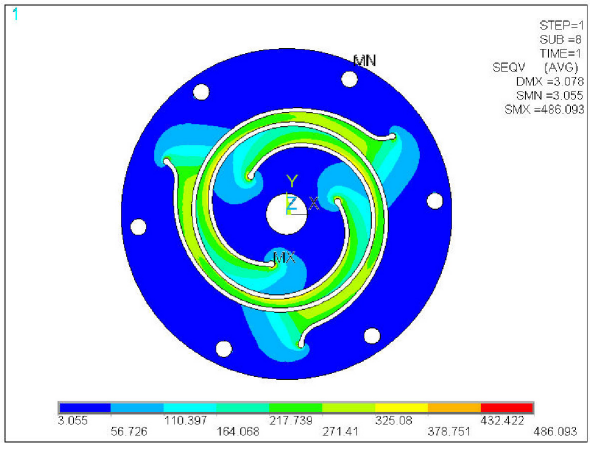

Figure 5. Stress distribution in the flexure element.

Table 1. Ratio of Radial Stiffness to Axial Stiffness

Displacement (mm)	Axial Stiffness (Ka) (N/m)	Radial Stiffness (Kr) (Avg.) (N/m)	Kr / Ka
1	770.82	46724.38	60.61
2	802.55	28330.08	35.30
3	853.50	16679.92	19.54

Assembly of System and Instrumentation

Displacements of the pistons are measured using calibrated linear variable differential transformer (LVDT). This LVDT (Micro-Epsilon, Germany) is specifically made Helium-tight at high pressures. Special care is taken to balance the moving masses of the two motors to reduce vibration in the dual opposed motor configuration.

The aluminum flange has a provision for a central gas discharge passage of about 2.5 mm in diameter. The central compression chamber is instrumented with an Endevco piezo-resistive transducer to measure the pressure amplitude and a Platinum sensor to measure temperature of the compression space in the front of pistons. The aluminum central flange is connected through copper fins to a chilled water tank which can maintain a sink temperature in the range of 288-300 K. Additional cooling coils are placed on the pressure vessel adjacent to the coil winding to reduce the heat input to the magnets and working gas. Temperatures of the pressure vessel surface and the coil are measured using thermocouples to control the operating temperatures and evaluate the efficiency of cooling circuit. The discharge port of the central flange is connected to the gas fill/vent pipelines and an additional dead volume, with pressure and temperature sensors. After assembly of the interconnecting flanges of the pressure vessel by metallic seals, the system is evacuated and qualified by a leak test with a mass spectrometer.

RESONANCE FREQUENCY OF LINEAR MOTOR COMPRESSOR

The linear motor compressor acts as a pressure wave generator of low pressure amplitude. Its resonance frequency can be evaluated by considering it as a first order spring mass system with low damping[3]. Neglecting damping, the resonance frequency f_{res} of the linear motor is expressed as:

$$f_{res} = (1/2\pi)\sqrt{K/m} \tag{2}$$

where K is the total spring stiffness.

$$K = K_s + K_m + K_g \tag{3}$$

where K_s is the flexure mechanical spring stiffness, K_m is the magnetic spring stiffness due to the magnetic restoring force and K_g is the gas spring stiffness

$$K_g = K_{gf} + K_{gb} \tag{4}$$

where K_{gf} is the spring stiffness of the gas volume in front of the piston and K_{gb} is the spring stiffness of the gas volume in the back side of the piston.

$$K_{gf} = P_m (A_c)^2 \gamma / V_{df} \tag{5}$$

$$K_{gb} = P_m (A_c)^2 \gamma / V_{db} \tag{6}$$

where P_m is the mean gas fill pressure, A_c is the cross sectional area of the piston, V_{df} is the gas dead volume in the compression space in front of the pistons, V_{db} is the gas dead volume in the back of the piston and γ is the ratio of specific heats.

In a linear motor compressor under the resonance conditions, the inertial forces of the moving mass will be cancelled by the mechanical, magnetic and gas spring forces acting in the opposite direction, thus requiring minimum input power to produce the designed PV work of the compressor. It is important to operate the linear motors in the resonance condition to minimize input electrical power. Precise estimation and optimization of the constituent components of spring mass equation has been carried out to achieve this goal.

EXPERIMENTS AND RESULTS

No Gas Load Testing of Linear Motors - Piston Exposed to Ambient Pressure

The motors alone (without cylinders) are run using a Chroma model 61502 AC source which can provide a pure sinusoidal current to the motor coils. The frequency is varied and the operating parameters of the motor in terms of input power, current, input voltage and power factor are measured by a Yokogawa power meter WT230. The coil resistance at operating temperature of the coil was also measured. Since the piston front and back are exposed to ambient pressure, no gas spring forces are present. Hence

$$f_{res}(\text{motor}) = (1/2\pi)\sqrt{(K_s + K_m)/m} \tag{7}$$

A resonance frequency of 53 Hz is recorded in the experiments and this matches the predicted value. Under the resonance conditions, the minimal input power is entirely consumed by the negligible copper losses and the rest by the iron losses comprising the hysteresis losses and eddy losses. By deducting the copper losses from the input power, the total iron losses for the motor at the operating frequency can be estimated. For motor A the iron loss is 0.58 Watts and for motor B the iron loss is 0.24 Watts. The higher losses for motor A could be attributed to a larger air gap in the magnetic circuit caused by manufacturing deviations. Hysteresis losses vary with frequency while eddy losses vary to the square of the frequency[4]. An upper bound value for iron losses at other operating frequencies can therefore be estimated by multiplying the basic motor iron loss by the square of frequency ratio. During the test at resonance, the motors A and B have recorded power factors of 0.90 and 0.94 respectively.

Operations at Different Gas Loads and using Different Diameter Transfer lines

The linear motor compressor is operated with Helium fill pressures of 10 bar, 15 bar, 20 bar and 25 bar at varying frequencies and using transfer lines of inner diameter 1.75 mm (V_{df} = 8.5 cc) and 3.25 mm (V_{df} = 11.6 cc). During each run apart from electrical power parameters, pressure amplitude P_v, LVDT displacement and phase angle ø between pressure and volume flow rate as well as the sink and coil temperatures are measured. Acoustic power and mass flow rates are evaluated from the experiments.

The acoustic power at the piston is given by the equation

$$\dot{W} = 2\pi f |p_v V| \cos(\phi) \tag{8}$$

The mass flow rate can be estimated from the equation

$$\dot{m} = (2\pi f |V| P_o)/(ZRT_o) \tag{9}$$

where R = specific gas constant of helium, T_o = Temperature of compression space = sink temperature, P_o = mean compressor gas fill pressure, Z = compressibility factor for helium($\simeq$1) and |V| is the amplitude of volume flow.

Figures 6(a) and 6(b) show the variation of total input power with operating frequency of the compressor at different gas fill pressures for nearly the same displacement amplitudes. From the plots it can be seen that a transfer line of 3.25 mm diameter results in lower input power as compared to a 1.75 mm diameter transfer line. It is also observed that for a motor with 327 turns, 18 SWG winding draws less input power compared to a 180 turns, 21 SWG winding coil even though both have the same resistance values. Therefore, it was concluded that 18 SWG wire is preferred for winding the motors.

Figure 7(a) shows the resonance frequency obtained from experiments and the theoretically estimated values for 1.75 mm diameter pipe line. The experimentally obtained resonance frequencies are

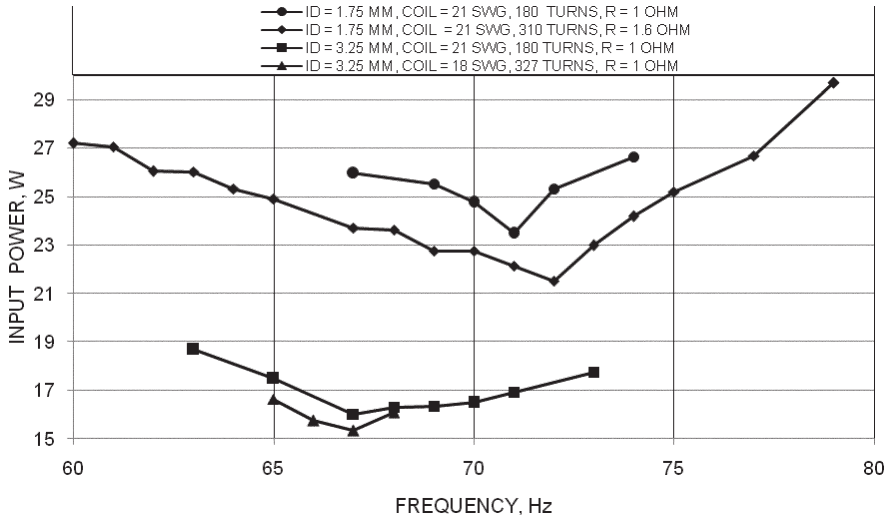

(a)

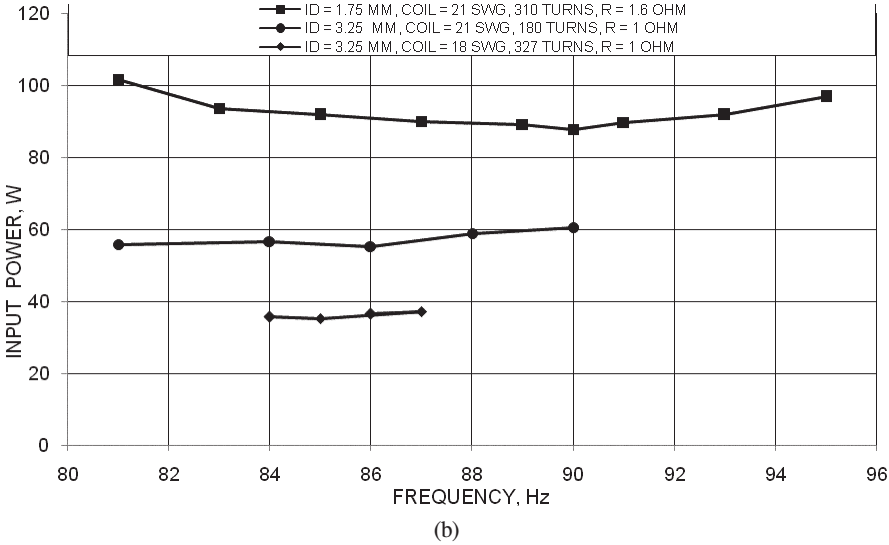

(b)

Figure 6. Total input power v/s operating frequency of the compressor at fill pressures of (a) 10 bar and (b) 25 bar specific to transfer line transfer line diameters, wire gauge, resistance and number of turns of the coil.

lower from the theoretical values by about 1 to 9 Hz, which indicates a reduction of gas spring force of the system for this transfer line diameter. Unfortunately at the present there is no transducer to measure the compressor back pressure and thus to assess variation in the back volume spring stiffness.

The resonance frequencies for different gas fill pressures for the 3.25 mm transfer line are shown in Fig. 7(b). In this case the theoretical resonance frequency matches very closely with the experimentally determined resonance frequencies, thus resulting in lower input power.

Table 2 gives the input power, copper loss, iron loss, shaft power (input power - copper loss-iron loss), shaft power efficiency (shaft power / input power) , measured acoustic power at the face of pistons, acoustic power efficiency (measured acoustic power / shaft power), pressure amplitude and mass flow rate for different fill pressures and corresponding resonance frequencies at a specific stroke amplitude. The following are the pertinent observations from the test:

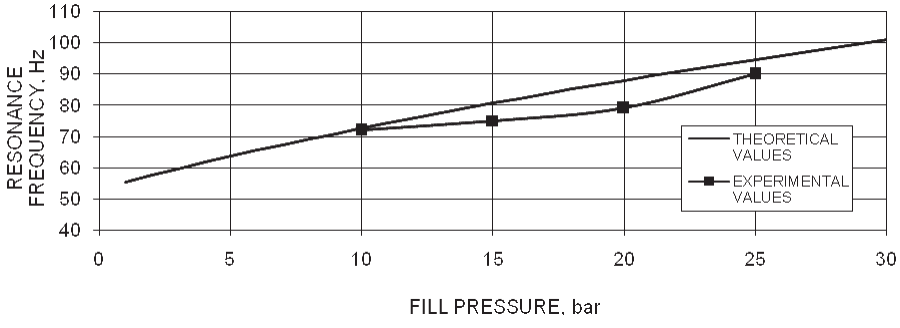

(a)

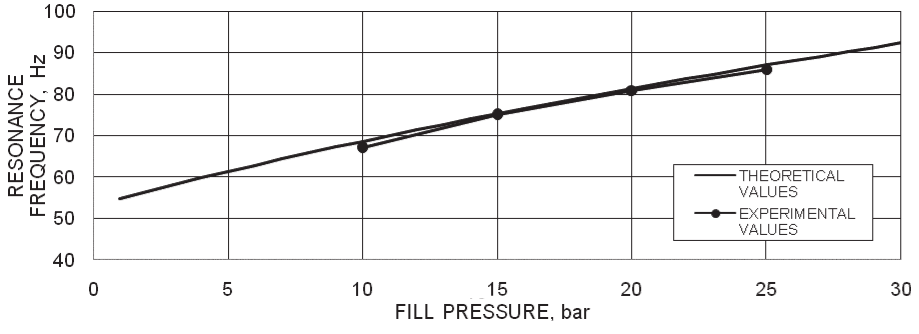

(b)

Figure 7. Theoretical and experimental values of the resonance frequencies at different fill pressures. (a) Transfer line diameter 1.75 mm and dead volume of 8.5 cc. (b) Transfer line diameter 3.25 mm and dead volume of 11.6 cc.

1. The measured acoustic power for a given input power shows significant increase for lager diameter transfer line (3.25 mm ID) as compared to smaller diameter transfer line (1.75 mm ID). This calls for more detailed future investigation to optimize the efficiency of the PWG with respect to the flow passage dimensions.
2. The shaft power for a given input power is much larger for 18 gauge coil winding as compared to 21 gauge wire of identical coil resistance values and transfer line dimensions.
3. At 25 bar fill pressure with 35.2 W of input power, the PWG has produced a shaft power of 26.82 W (76% efficiency). However out of 26.82 W of shaft power, only 18.7 W (70% efficiency) has been obtained as acoustic power at the compression space. The measured acoustic power is lower than the shaft power, since a part of the input power is lost through blowby losses and irreversible heat transfer between compressed gas and compressor physical entity and pressure drop losses in the flow passages.
4. There is considerable scope to increase the acoustic power by cutting down mechanical losses especially the blowby losses at the piston-cylinder clearance seal through improved design and its implementation by precision fabrication and assembly.
5. An acoustic power of 18.7 W with an input power of 35.2 W should be able to produce refrigeration power greater than 1 W at 77 K in a high frequency pulse tube cooler of matching acoustic load. Therefore a development program for a matching high frequency pulse tube cooler can be taken up.

CONCLUSIONS

In the first developmental effort undertaken, a compact moving magnet pressure wave generator has been built providing an acoustic power of 18.7 W, pressure amplitude of 1.8 bar and mass

Table 2. Performance Chart of Pressure Wave Generator

P_o	f_{res}	Stroke amplitude	Input power	Copper loss	Iron loss max.	Shaft power	Shaft power efficiency	$\dot{w}$	Acoustic power efficiency	P_v	$\dot{m}$
bar	Hz	mm	W	W	W	W	%	W	%	bar	g/s
Transfer line ID =1.75 mm, coil = 310 turns (21 SWG), R = 1.6 ohm and sink temperature = 298 K											
10	72	1.8	21.51	5.35	1.51	14.65	68	9.3	63	1.0	0.33
15	75	1.9	34.95	10.46	1.64	22.85	65	13.6	60	1.4	0.53
20	79	1.8	60.56	20.75	1.82	37.99	63	18.4	49	1.9	0.71
25	90	1.9	87.92	28.93	2.36	56.63	64	28.1	50	2.2	1.07
Transfer line ID = 1.75 mm, coil = 180 turns (21 SWG), R = 1 ohm and sink temperature = 298 K											
10	71	1.9	23.48	8.83	1.47	13.17	56	9.1	69	1.0	0.34
15	75	1.8	45.27	19.91	1.64	23.72	52	14.1	59	1.4	0.52
Transfer line ID = 3.25 mm , coil = 180 turns (21 SWG), R = 1 ohm and sink temperature = 298 K											
10	67	1.9	16.02	5.49	1.31	9.22	58	7.2	78	0.9	0.32
15	75	1.8	23.19	8.23	1.64	13.32	57	11.1	83	1.2	0.52
20	81	1.8	35.29	13.58	1.92	19.79	56	15.6	79	1.5	0.73
25	86	1.8	55.38	22.84	2.16	30.39	55	21.9	72	1.9	0.99
Transfer line ID = 3.25 mm, coil = 327 turns (18 SWG), R = 1 ohm and sink temperature = 298 K											
10	67	2.0	15.34	2.26	1.17	11.92	78	8.6	72	0.89	0.34
15	75	2.2	31.43	4.78	1.64	25.01	80	17.8	71	1.50	0.63
20	79	1.9	33.76	5.76	1.82	26.17	78	18.5	71	1.68	0.77
25	85	1.7	35.20	6.27	2.11	26.82	76	18.7	70	1.80	0.93

flow rate of 0.93 g/s with an input power of about 35.2 W. Future efforts will include improving the performance by cutting down on the mechanical losses of the compressor.

ACKNOWLEDGMENTS

The work was supported by ISRO/RESPOND. The authors appreciate the help given by ISAC Bangalore, Sandvik (India/Sweden) and Höganäs (India/Sweden) for the specific material support for the program, the staff of the Centre for Cryogenic Technology for providing the dedicated water chiller for the experiments and their help in setting up the test facility, and Dr. John Corey and Dr. Srinivas Vanapalli for useful discussions.

REFERENCES

1. Matsumoto, N., Yasukawa, Y., Ohshima, K., Takeuchi, T., Matsushita, T., Mizoguchi, Y., "Development of a compressor for a miniature pulse tube cryocooler of 2.5 W at 65 K for telecommunication applications," *Adv. in Cryogenic Engineering*, Vol. 53, Amer. Institute of Physics, Melville, NY (2008) pp. 1100-1107.
2. Beale et.al., "Linear generator or motor with integral magnetic spring," U.S. Patent, 5148066, September 15, 1992.
3. Corey et al., "Matching an acoustic driver to an acoustic load in an acoustic resonant system," U.S Patent 6604363, August 12, 2003.
4. Mai, M., Ruehlich, I., Rosenhagen, C., Wiedmann, Th., "Development of Miniature Flexure Bearing Cryocooler SF070," *Cryocoolers 15*, ICC Press, Boulder, CO (2009), pp. 133-138.